Theoret. Chim. Acta (Berl.) 43, 337–349 (1977)

THEORETICA CHIMICA ACTA

Ab initio SCF and CI Study of the Electronic Spectrum of Pyridine N-Oxide

Tae-Kyu Ha

Laboratory of Physical Chemistry, Swiss Federal Institute of Technology, Zürich, Switzerland

Configuration interaction (CI) studies of ground, $n \rightarrow \pi^*$, $\pi \rightarrow \pi^*$ electronically excited states are reported for pyridine N-oxide. The transition energy to the lowest $\pi \rightarrow \pi^*$ excited $^1B_2$ state is calculated at 4.35 eV, compared to the experimental spectrum range of 3.67–4.0 eV. This state lies below the lowest $n \rightarrow \pi^*$ excited $^1A_2$ state calculated at 4.81 eV above the ground state. The only experimentally reported triplet state at 2.92 eV above the ground state is predicted to be the $^3A_1$ ($\pi\pi^*$) state. The calculated energy lies at 3.27 eV. Numerous other high-lying singlet states as well as the triplet states have also been calculated. The intramolecular charge transfer character of the ground and the excited states have been studied in terms of the calculated dipole moment and other physical properties.

Key words: Pyridine N-Oxide, electronic spectrum of ~

1. Introduction

Heterocyclic amine N-oxides are of interest with respect to their biological and photochemical importance associated with some of the naturally occurring organic species [1]. Pyridine N-oxide is the simplest member of the heterocyclic N-oxides which contain the N-O group acting as a donator-acceptor [1, 2].

The molecular structure of pyridine N-oxide has recently been determined by gas phase electron diffraction [3] and by microwave studies [4]. The ionization energies have also been determined by photoelectron spectroscopy [5, 6]. The UV spectrum has been measured by various groups [7–11]. Four electronic transitions have been reported for pyridine N-oxide. A weak transition ($f = 0.012$) at 320 mμ and three moderately strong transitions at 280 mμ ($f = 0.173$), at 215 mμ ($\epsilon_{max} = 18\,000$) and at 188 mμ ($f = 0.25$). There is no definitive assignment for any of these states. The 320 mμ transition, for example, has been originally described to be the first $n \rightarrow \pi^*$ transition. This assignment, however, was questioned by various people. Several semi-empirical MO studies [7, 11, 12–14] have also been carried out to interpret the electronic transition, with conflicting results, depending upon the employed semi-empirical parameters and the approximations involved. The conflict in the above assignments warrants a more thorough theoretical examination of the spectral features of this photochemically interesting molecule.

In this work we report an *ab initio* SCF and CI study of the ground and various electronically excited states of pyridine N-oxide. Since pyridine N-oxide may be regarded as an intramolecular charge transfer complex between pyridine and an oxygen atom, it is expected that the ground state as well as various electronically excited states would have varying degrees of charge transfer properties. These will be studied in terms of the calculated dipole moment for the state of interest.

2. Calculation

Ab initio SCF calculations have been carried out for pyridine N-oxide employing two different choices of Gaussian basis sets. The approximate Hartree-Fock SCF atomic orbitals used as a basis set in the calculation were the Gaussian lobe functions [15]. The first basis set (basis set I) consists of three linear combinations of four, three and three primitive Gaussians for *s*-orbitals and one contraction of five pairs of Gaussians for each of the three *p*-orbitals of carbon, nitrogen and oxygen atoms. Each hydrogen *s*-orbital was represented by a linear combination of five primitive Gaussians scaled by a factor of $2^{1/2}$ [16]. The second basis set (basis set II) is a slightly extended one, in which additional one-term long-range p_π functions of the same exponents and lobe separations as the most diffuse *p*-function of C, N and O were added to the basis set I. The total basis set thus contains 95 *s*-type Gaussians and 105 *p*-type (basis set I) or 112 *p*-type (basis set II) Gaussian functions, where a single *p*-function consists, in turn, of two symmetrically located spherical Gaussians. This size of the atomic basis set is approximately equivalent to the double-zeta Slater type orbital basis set in accuracy [15].

Bond distances and bond angles were taken from the experimental value of Ref. [3]. Table 1 summarizes the atomic coordinates in pyridine N-oxide, which are adopted for the calculation. Table 2 summarizes molecular energies obtained from the ground-state SCF calculations for two different basis sets. MO's with their symmetries are also listed.

As noticed in Table 2 the molecular SCF energy for the basis set I is lowered by only 0.0302 a.u. as a result of the addition of the long-range p_π-functions to the basis set I. However, the essential point of interest is that the basis set II is considered much more

Table 1. Coordinates of atoms in pyridine N-oxide[a]

	x	*y*
N	0.0000	0.000
O	0.0000	−2.4378
C_1	2.2764	1.2879
C_2	−2.2764	1.2879
C_3	2.2764	3.8976
C_4	−2.2764	3.8976
C_5	0.0000	5.3312
H_1	4.0274	0.2906
H_2	−4.0274	0.2906
H_3	4.0533	4.8625
H_4	−4.0533	4.8625
H_5	0.0000	7.3532

[a] Atomic units

Table 2. Molecular orbitals and total energies from ground-state SCF calculation on pyridine N-oxide for two different basis sets[a]

φ	Orbital Symmetry	Basis Set I[b]	Basis Set II[b]
1	$1a_1$	−20.4522	−20.4996
2	$2a_1$	−15.8689	−15.8550
3	$1b_2$	−11.4284	−11.4206
4	$3a_1$	−11.4284	−11.4206
5	$4b_2$	−11.4080	−11.3952
6	$4a_1$	−11.4080	−11.3952
7	$5a_1$	−11.3841	−11.3821
8	$6a_1$	−1.4660	−1.4674
9	$7a_1$	−1.2260	−1.2259
10	$3b_2$	−1.1113	−1.1074
11	$8a_1$	−1.1025	−1.1011
12	$4b_2$	−0.9279	−0.9237
13	$9a_1$	−0.9115	−0.9088
14	$10a_1$	−0.7665	−0.7651
15	$5b_2$	−0.7443	−0.7405
16	$11a_1$	−0.7213	−0.7183
17	$6b_2$	−0.6789	−0.6846
18	$1b_1$	−0.6758	−0.6753
19	$12a_1$	−0.6479	−0.6492
20	$7b_2$	−0.5857	−0.5821
21	$13a_1$	−0.5782	−0.5777
22	$2b_1$	−0.5098	−0.5129
23	$8b_2$	−0.4356	−0.4414
24	$1a_2$	−0.4302	−0.4360
25	$3b_1$	−0.3211	−0.3281
Total energy		−321.0184	−321.0486

[a] Atomic units.
[b] For definition of basis set see text.

flexible as far as the π-orbitals are concerned. This basis set (basis set II) provides among other things a larger set of virtual orbitals, which can be transformed to an optimal set of π^*-orbitals to be used for the CI treatment of the ground, $n\pi^*$ and $\pi\pi^*$ singlet and triplet excited states as discussed below. From the SCF ground-state calculation employing the basis set II, 25 occupied φ_1-φ_{25} (e.g. Table 2) and 29 virtual orbitals were obtained. Prior to the multistep CI treatment [17-22], a truncation of certain molecular orbital bases is unavoidable because of limitations in the computational capabilities. First, those virtual orbitals to the ground-state orbital energies greater than ~200 a.u. (seven such orbitals) are discarded, since such virtual orbitals, which are thought to be unimportant in the description of bonding, arise as a consequence of the inclusion of the short-range (cusp) functions in the Gaussian basis set. Among ground-state SCF occupied orbitals, six higher-lying MO's, φ_{20}-φ_{25} are selected as orbitals of variable occupancy. The remaining virtual orbitals have been transformed in such a way that the sum of exchange integrals between these and the

variable set of the occupied orbitals, φ_{20}-φ_{25}, was a maximum;

$$I = \sum_{i=20}^{25} \left\langle \varphi_v(1)\varphi_i(1) \left| \frac{1}{r_{12}} \right| \varphi_v(2)\varphi_i(2) \right\rangle = \text{max.}$$

with $\langle \varphi_v | \varphi_i \rangle = \delta_{vi}$, where $\varphi_v = \Sigma_{k=26}^{47} c_{vk}\varphi_k$, $v = 26, \ldots 47$, is a linear combination of the SCF ground-state virtual orbitals and φ_i are the occupied set of variable orbitals. The use of such transformed virtual orbitals obtained in this way proved to be useful in obtaining better convergence using a limited number of configurations in the CI treatment [19-22]. Among these 22 transformed virtual orbitals, 10 orbitals (8 π* type and 2 σ* type) were selected to be used to build configurations. Thus, we actually included 16 orbitals of variable occupancy for generating configurations.

Table 3 summarizes these orbitals along with symmetries and orbital energies. It is to be noted that the transformed virtual orbital energies are negative as opposed to the positive energies of the usual SCF virtual orbitals.

A multistep CI calculation was carried out by generating configurations referenced to a particular state of interest. In the first step a small number of configurations $\Psi_I^{(1)}$, which was judged to be important for a qualitative description of the state of interest, was chosen. This set was augmented by all configurations $\Psi_J^{(2)}$ which were singly and doubly excited with respect to all members of the parent set and which fulfilled the following interaction criterion with the parent set;

$$\frac{|\langle \Psi_I^{(1)} | H | \Psi_J^{(2)} \rangle|^2}{|E_I^{(1)} - E_J^{(2)}|} > \delta$$

with $\delta = 10^{-3}$ as the energy threshold.

The resulting Hamiltonian matrix was diagonalized and the energy E_I' and the wave function Ψ_I',

$$\Psi_I' = \sum_m [d_{mI}^{(1)}\Psi_m^{(1)} + d_{mI}^{(2)}\Psi_m^{(2)}]$$

Table 3. Energies and symmetries of orbitals of variable occupancies used to build configurations[a]

Orbital	Symmetry	ϵ_i (a.u.)	Orbital	Symmetry	ϵ_i (a.u.)
20	$7b_2$ (σ)	−0.5821	28	$5b_1$ (π*)	−0.1751
21	$13a_1$ (σ)	−0.5777	29	$14a_1$ (σ*)	−0.1327
22	$2b_1$ (π)	−0.5129	30	$9b_2$ (σ*)	−0.1032
23	$8b_2$ (η)	−0.4414	31	$6b_1$ (π*)	−0.0942
24	$1a_2$ (π)	−0.4360	32	$7b_1$ (π*)	−0.0832
25	$3b_1$ (π)	−0.3281	33	$3a_2$ (π*)	−0.0635
26	$4b_1$ (π*)	−0.3008	34	$4a_2$ (π*)	−0.0588
27	$2a_2$ (π*)	−0.2094	35	$8b_1$ (π*)	−0.0289

[a] For basis set II. The virtual orbitals, φ_{26}-φ_{35} were determined by the exchange maximization with the occupied SCF orbitals, φ_{20}-φ_{25} (see text).

were obtained. In the second step the set of wave functions Ψ_I' obtained by the above procedure was considered to build a new parent set. Again, this set was augmented by all singly and doubly excited configurations which have an interaction energy threshold greater than $\delta = 10^{-5}$. Within this energy threshold convergence was obtained within about 300 configurations for describing the ground and $n\pi^*$, $\pi\pi^*$ electronically excited states of interest.

Table 4 summarizes energies of pyridine N-oxide in the ground state and several electronically excited singlet and triplet states before and after the CI treatment. For example, the SCF ground-state energy of −321.0486 a.u. is lowered by 0.0802 a.u. in the first step including 36 configurations and by an additional 0.0179 a.u. in the second step which involved 135 configurations giving ground-state CI energy of −321.1467 a.u. Single configuration energies for the excited states included in Table 4 are understood to be those energies which correspond to certain configurations due to orbital promotions, and which were not further optimized. These are calculated via expectation values, not via Roothaan's open-shell treatment. It is also evident that the CI treatment

Table 4. Energies of pyridine N-oxide ground and electronically excited states based on ground-state SCF orbitals and transformed virtual orbitals (atomic units)

Electronic State	Single Configuration Energy (Orbital Promotion)	First Step $\delta = 10^{-3}$ (Number of Configuration Considered)	Final Step $\delta = 10^{-5}$ (Number of Configuration Considered)	Qualitative Description of Transition
$^1A_1$	−321.0486	−321.1288 (36)	−321.1467 (135)	Ground state
$^1B_2$	−320.7574 (25 → 27)	−320.9523 (42)	−320.9868 (224)	$\pi \rightarrow \pi^*$
$^1A_2$	−320.7624 (23 → 26)	−320.9435 (35)	−320.9700 (262)	$n \rightarrow \pi^*$
$^1A_1$	−320.7102 (25 → 26)	−320.9385 (39)	−320.9622 (221)	$\pi \rightarrow \pi^*$
$^1A_1$	−320.5861 (25 → 28)	−320.8541 (54)	−320.9077 (258)	$\pi \rightarrow \pi^*$
$^1B_1$	−320.6342 (23 → 27)	−320.7868 (39)	−320.8137 (224)	$n \rightarrow \pi^*$
$^1A_1$	−320.6973 (24 → 27)	−320.7725 (42)	−320.8001 (213)	$\pi \rightarrow \pi^*$
$^3A_2$	−320.7750 (23 → 26)	−320.8627 (35)	−320.8932 (235)	$n \rightarrow \pi^*$
$^3A_1$	−320.8354 (25 → 26)	−320.9900 (41)	−321.0266 (252)	$\pi \rightarrow \pi^*$
$^3B_2$	−320.7893 (25 → 27)	−320.8786 (35)	−320.9056 (212)	$\pi \rightarrow \pi^*$
$^3A_1$	−320.7840 (24 → 27)	−320.8974 (41)	−320.9065 (213)	$\pi \rightarrow \pi^*$

strongly influences electronically excited states as shown in the table. A qualitative description of the transition from which excited states are built is also given.

The final CI wave functions for the ground and excited states which correspond to those energies shown in Table 4 are summarized in Table 5. We have listed only those important configurations whose coefficients are larger than 0.1 in magnitude.

3. Discussion

3.1. Ground-State Properties

Before discussing the electronic spectrum in detail it is worthwhile to briefly summarize some of the ground-state properties of pyridine N-oxide obtained from the SCF calcu-

Table 5. Major contribution to the ground and excited state CI wave function of pyridine N-oxide[a]

Configurations	$^1A_1$	$^1A_1$	$^1A_1$	$^1A_1$	$^3A_1$	$^3A_1$
Ground state	0.95					
$25^2 \rightarrow 26^2$	0.17	0.22		0.32		
$24^2 \rightarrow 27^2$	0.11					
$24, 25 \rightarrow 26, 27$	0.10			0.30		
$25 \rightarrow 26$		0.56	0.41	0.15	0.62	0.12
$25 \rightarrow 31$		0.35	0.16	0.22	0.30	
$25 \rightarrow 28$		0.20	0.11	0.51	0.12	0.14
$22, 25 \rightarrow 26^2$		0.12		0.22		
$24 \rightarrow 27$		0.13	0.55		0.12	0.62
$25^2 \rightarrow 26, 28$		0.10		0.20		
$25^2 \rightarrow 26, 31$		0.13				
$22 \rightarrow 26$		0.13		0.43		
$24 \rightarrow 34$				0.34		0.34
Configurations	$^1B_2$	$^1A_2$	$^1B_1$	$^3B_2$	$^3A_2$	
$25 \rightarrow 27$	0.59			0.88		
$25 \rightarrow 34$	0.30			0.26		
$25^2 \rightarrow 26, 27$	0.20			0.15		
$22, 25 \rightarrow 26, 27$	0.13			0.24		
$25^2 \rightarrow 27, 28$	0.11					
$24 \rightarrow 26$	0.24			0.10		
$24, 25 \rightarrow 27^2$	0.10					
$23 \rightarrow 26$		0.61			0.90	
$23 \rightarrow 31$		0.30			0.25	
$23, 25 \rightarrow 26^2$		0.27			0.23	
$23, 24^2 \rightarrow 26, 27^2$		0.10				
$23, 25 \rightarrow 26, 31$		0.11				
$23 \rightarrow 27$			0.87			
$23, 25 \rightarrow 26, 27$			0.22			
$23 \rightarrow 34$			0.24			
$23, 24 \rightarrow 26^2$			0.13			

[a] Only those configurations with coefficients larger than 0.1 in magnitude in the final CI wave functions are listed.

lation. Since pyridine N-oxide may be regarded as a weakly bonded intramolecular charge transfer complex between pyridine and an oxygen atom, the charge transfer properties of the ground state can be discussed by comparing the molecular properties referenced to the pyridine molecule. Values for pyridine were taken from Refs. [23, 24], which employed the same size of Gaussian basis set as basis set I of this work.

Fig. 1 shows the σ-charge density contour diagram of pyridine N-oxide, which may be compared with Fig. 1 of Ref. [24] for pyridine. The electronic populations in pyridine N-oxide are summarized in Table 6 and are compared with those of pyridine. Inspecting the atomic orbital population in detail, it is noted that oxygen withdraws σ electrons mostly from the nitrogen, while it donates π electrons to the ring via nitrogen. In this sense, pyridine N-oxide may be regarded as two-way donor-acceptor intramolecular

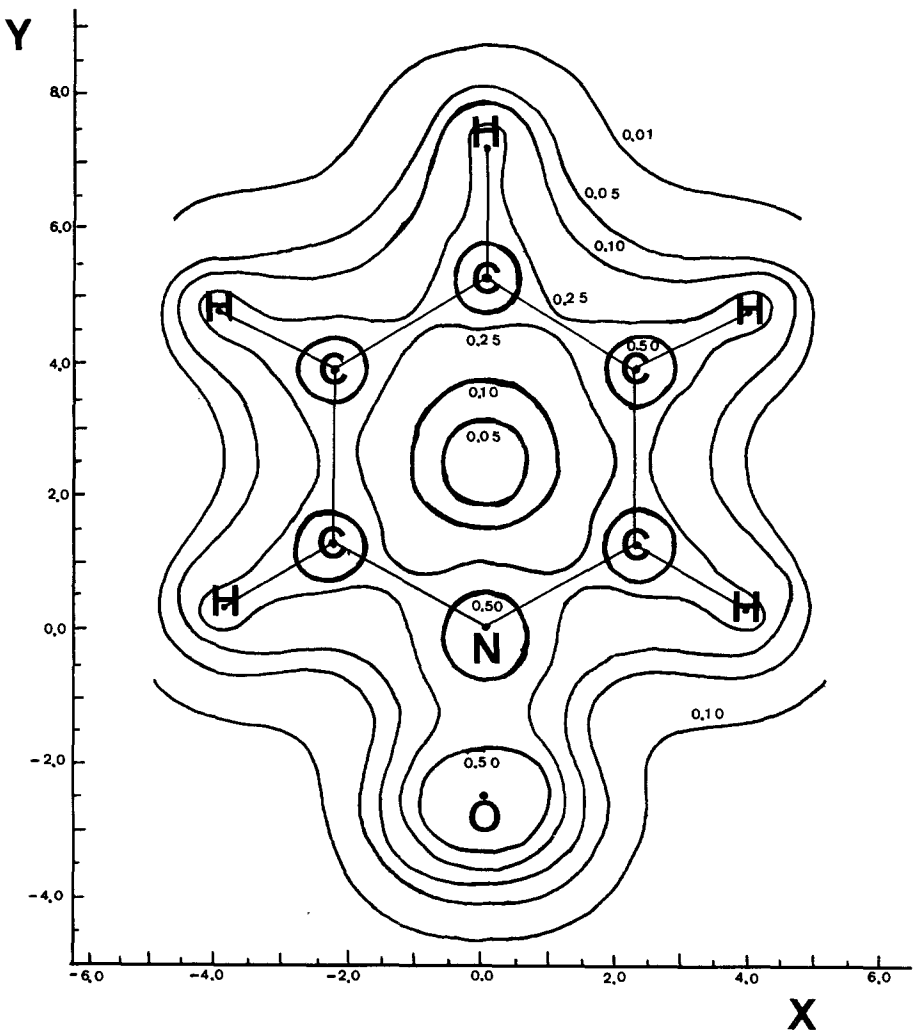

Fig. 1. σ-Charge density contour diagram for pyridine N-oxide (a.u.)

Table 6. Electron populations in pyridine and pyridine N-oxide

		Pyridine	Pyridine N-Oxide
N	s	3.605	3.435
	p_σ	2.584	2.232
	p_π	0.933	1.255
	Total	7.122	6.922
O	s		3.917
	p_σ		2.852
	p_π		1.393
	Total		8.162
C_1 (=C_2)	s	3.150	3.121
	p_σ	1.892	1.811
	p_π	1.054	1.188
	Total	6.096	6.120
C_3 (= C_4)	s	3.160	3.166
	p_σ	2.006	2.020
	p_π	0.979	0.931
	Total	6.145	6.117
C_5	s	3.167	3.150
	p_σ	1.969	1.926
	p_π	1.001	1.114
	Total	6.137	6.190
H_1 (= H_2)	s	0.848	0.839
H_3 (= H_4)	s	0.855	0.854
H_5	s	0.851	0.865

complex such as borine carbonyl (BH_3CO), in which the stabilization was considered to be partially due to the back donation of π charges from BH_3 to CO, the σ charge transfer from CO to BH_3 being the main source of the formation of the complex [25, 26]. This work thus supports the experimental findings [25] that pyridine in pyridine N-oxide is an amphodonor (σ-donor and π-acceptor) toward the oxygen atom, whereas the oxygen atom is an amphoceptor (σ-acceptor and π-donor).

The calculated dipole moment of 4.64 D (expt., 4.2 D [7]) is much larger than 2.6 D (expt. 2.21 D [24]) for pyridine. The nuclear quadrupole coupling constants (eQq_{mol}) have been calculated in the field gradient principal axis system employing the quadrupole moment of $Q(^{14}N) = 1.56 \times 10^{-26}$ cm^2 [27] and $Q(^{17}O) = 2.63 \times 10^{-26}$ cm^2 [28]. We obtained values of 0.612 MHz with asymmetry parameter, $\eta = 0.809$ for ^{14}N and of 26.567 MHz with $\eta = 0.616$ for ^{17}O in pyridine N-oxide. It should be noted that for ^{14}N the largest component of the quadrupole coupling constant lies in the perpendicular axis to the molecular plane (z-axis), while for ^{17}O the largest component lies in the molecular plane (xy-plane). The eQq_{mol} value of 0.612 MHz for ^{14}N is considered to be extremely small compared to those of other heterocyclic compounds such as pyrrole, pyrazole, imidazole and pyridine, in which eQq_{mol} values are usually larger than 2 MHz. This small eQq_{mol} value is associated with the almost complete delocalization of the nitrogen "lone pair" orbital. On the other hand, the oxygen "lone pair"

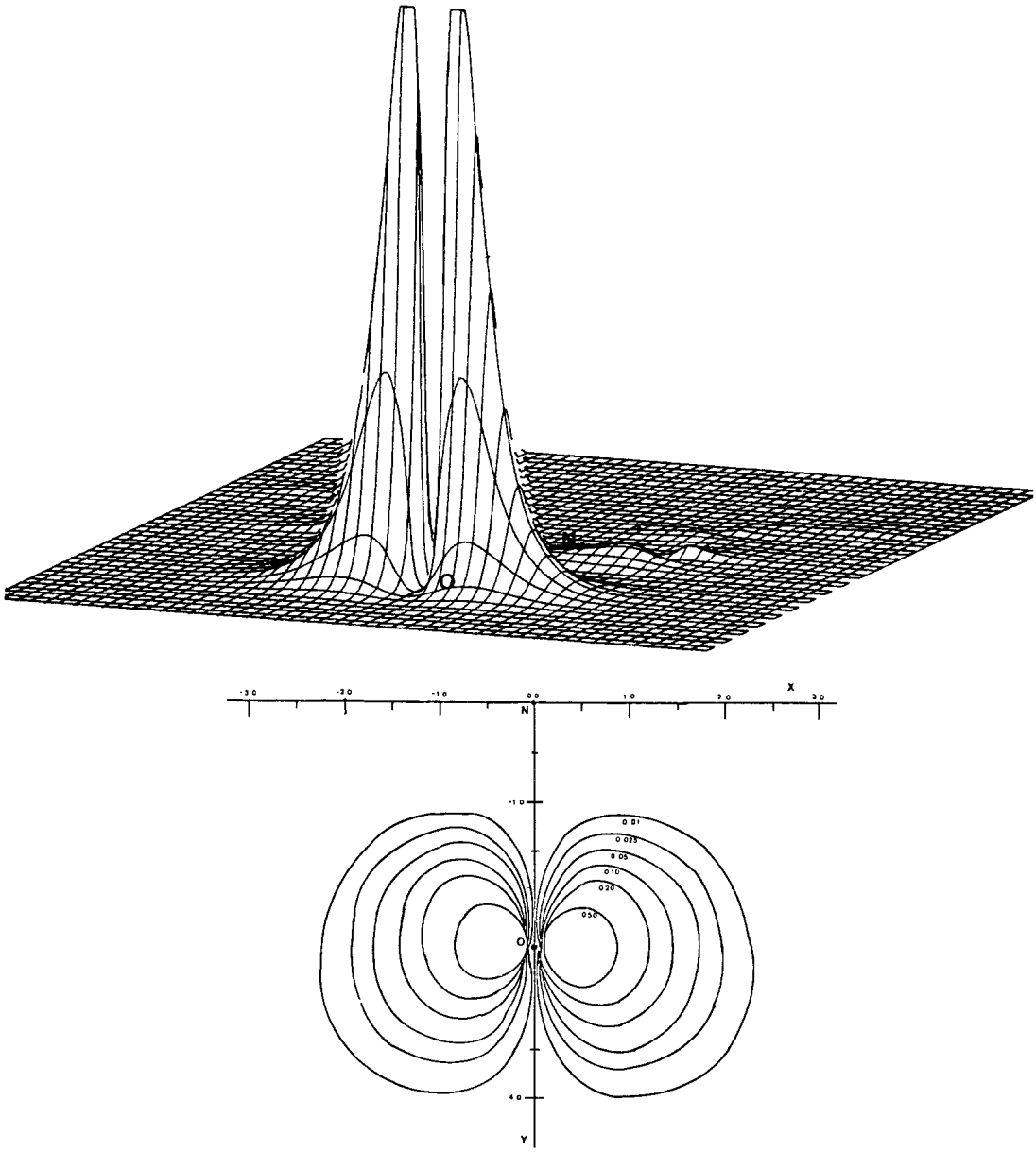

Fig. 2. Oxygen "lone pair" orbital ($8b_2$ MO) of pyridine N-oxide (a.u.)

orbital ($8b_2$ MO, e.g. Table 2), which is shown in Fig. 2 is almost localized at the oxygen atom. This highly localized MO is mainly responsible for the unusually large value of the oxygen eQq_{mol} of 26.567 MHz.

Comparing the valence shell MO's between pyridine and pyridine N-oxide it is noted that all MO's in pyridine N-oxide are lower in energy than the corresponding MO's of

pyridine. Three MO's, $3b_1$, $8b_2$ and $12a_1$, are of special interest. Judging from the LCAO coefficients these MO's may be regarded as characteristic MO's of pyridine N-oxide without having counterparts of the pyridine molecule. The photoelectron spectrum of pyridine N-oxide has been reported by Weiner and Lattman [6] and Maier and Muller [5]. For the assignments of the first and second ionization processes, the two reported experimental works are contradictory. While Weiner and Lattman assigned the first band to the ionization from the highest occupied σMO ($8b_2$ MO), which is highly localized on the oxygen [6], Maier and Muller assigned it to the highest occupied πMO ($3b_1$ MO). Within Koopmans' theorem the present *ab initio* SCF calculation supports the assignment made by Maier and Muller as far as the ordering of the energy levels is concerned.

3.2. Electronic Spectrum

Table 7 summarizes the calculated transition energies, dipole moments and the oscillator strengths of pyridine N-oxide and compares with available experimental values.

The transition from the ground state to the first excited singlet state is calculated at 4.35 eV, which is close to the experimental spectrum range of 6.37–4.0 eV. This transition has originally been assigned to a $n \rightarrow \pi^*$ transition largely on the basis of its blue shift characteristics in polar solvents. As shown in Table 5 this state, $^1B_2$ state, contains the dominant configuration which involves a promotion of an electron from the 25th MO (b_1 type πMO) to the 27th MO (a_2 type π^*MO) with a coefficient of 0.59. This $^1A_1 \rightarrow {}^1B_2$ ($\pi\pi^*$) transition is polarized in the molecular plane along the short axis. The LCAO coefficients for some higher-lying π-orbitals and lower-lying π^*-orbitals are shown in Table 8.

Table 7. A summary of calculated transition energies, dipole moments and oscillator strengths of pyridine N-oxide and comparison with available experimental values

Electronic State and Orbital Promotion	Dipole Moment (Debye)		Transition Energies (eV)		Oscillator Strength	
	Calc.	Expt.	Calc.	Expt.	Calc.	Expt.
$^1A_1$ (ground state)	4.29 4.64 (SCF)	4.2				
$^1B_2$ ($\pi\pi^*$)	3.20	3.5; 1.4	4.35	3.67–4.0	0.02	0.012
$^1A_2$ ($n\pi^*$)	1.05		4.81		~0.0	
$^1A_1$ ($\pi\pi^*$)	3.80	3.0	5.02	4.43	0.32	0.173
$^1A_1$ ($\pi\pi^*$)	2.63		6.50	5.77	0.35	0.196
$^1B_1$ ($n\pi^*$)	0.78		9.06		$\sim 10^{-4}$	
$^1A_1$ ($\pi\pi^*$)	3.25		9.43	6.60	0.40	0.240
$^3A_2$ ($n\pi^*$)	2.59		6.90			
$^3A_1$ ($\pi\pi^*$)	4.09		3.27	2.92		
$^3B_2$ ($\pi\pi^*$)	3.68		6.56			
$^3A_1$ ($\pi\pi^*$)	3.59		6.53			

Due to the pronounced lone pair character of the 23rd MO (n-orbital, e.g. Table 2), which is highly localized at the oxygen atom as shown in Fig. 2, the lowest $n \rightarrow \pi^*$ transition calculated at 4.81 eV above the ground state is strongly forbidden as the calculated oscillator strength value shows (f is almost zero). The lowest $n\pi^*$ state ($^1A_2$) lies slightly above the first $\pi\pi^*$ ($^1B_2$) state.

The strong electronic transition in the 280 mμ region reported in the literature is assigned to be the $^1A_1 \rightarrow {}^1A_1$ ($\pi\pi^*$) transition. The calculated transition energy of 5.02 eV lies slightly higher than the experimental value. According to Table 8 this transition has the dominant configuration which involves a promotion of an electron from the 25th MO to the 26th MO (b_1 type π^*MO) with a coefficient of 0.56. The transition is polarized in the molecular plane along the long axis (N-O axis) as the LCAO coefficients in Table 8 indicate.

While these two $\pi\pi^*$ states ($^1B_2$ and $^1A_2$ states) may be regarded as charge transfer states, the transition bands at 5.7 eV and 6.6 eV reported in the literature may be assigned to correspond to the ^1L_b and ^1L_a bands of pyridine, respectively. The calculated energies at 6.50 eV and 9.43 eV lie considerably higher than the experimental values. Two reasons seem to be responsible for the discrepancy between the calculated and the experimental values. First, the CI optimum orbitals in the higher excited states may be considerably more diffuse than could be achieved by distorting the valence shell atomic orbitals used in the present basis set. Second, a more significant variation in the inner shell orbitals might be required than is attainable in the present CI treatment which assumes a relatively large core of unperturbed ground-state SCF orbitals in the construction of excited states wave functions. It is expected that this effect may be more

Table 8. Comparison of π and π^* CI orbitals[a]

	$1a_2\pi$ (24)	$3b_1\pi$ (25)	$4b_1\pi^*$ (26)	$2a_2\pi^*$ (27)	$5b_1\pi^*$ (28)
N		−0.1835	0.5330		0.2369
O		0.6702	−0.8667		−0.3512
		0.1273(d)	0.5787(d)		0.3585(d)
C_1	0.4887	−0.3398	−0.3921	0.6930	−0.4818
				−0.2664(d)	0.1720(d)
C_2	−0.4887	−0.3398	−0.3921	−0.6930	−0.4818
				0.2664(d)	0.1720(d)
C_3	0.4326	0.1046	−0.2354	−0.7508	0.7088
				0.2924(d)	−0.3090(d)
C_4	−0.4326	0.1046	−0.2354	0.7508	0.7088
				−0.2924(d)	−0.3090(d)
C_5		0.4089	0.6048		−0.8453
			−0.1680(d)		0.4187(d)

[a] Coefficients of carbon, nitrogen and oxygen p_π basis functions are tabulated, which are larger than 0.1 in magnitude; subscript d denotes the long range p_π group.

significant in case highly diffuse π-orbitals are involved in the description of the excited states.

In addition to the singlet manifold, several low-lying triplet states have also been calculated. Among these calculated states the transition $^1A_1 \rightarrow {}^3A_1$ ($\pi\pi^*$) with 3.27 eV is the only one observed experimentally. The experimental transition energy is reported at 2.92 eV [29].

The calculated electric dipole moment of the ground and various excited states provides a measure of the electron transfer. The dipole moment value of 4.64 D in the SCF level of the calculation was improved to 4.29 D in the CI treatment, which is in excellent agreement with the experimental value of 4.2 D. The change in dipole moment on electron excitation, $^1A_1 \rightarrow {}^1B_2$ (the first excited singlet state) is calculated as around 1 D. Experimentally two considerably conflicting values have been reported in the literature concerning the change in the dipole moment for the $^1A_1 \rightarrow {}^1B_2$ transition. Seibold *et al.* [7] reported a value of 2.8 D obtained from electrodichromic experiments. Hochstrasser and Wiersma [10], on the other hand, reported a value of 0.7 D obtained from Stark effect measurements. The present calculation gives a value which lies close to the latter, meaning that the electron transfer from oxygen to the ring in the excited $^1B_2$ state is much smaller than predicted by electrochromic measurements. Various semi-empirical MO calculations [7, 13, 14] also overestimated the electron transfer considerably.

Acknowledgements. We express our appreciation to the ETH Zürich computer centre for providing computer time and Professor Hs. H. Günthard for his encouragement and advice.

References

1. Ochiai, E.: Aromatic amine oxide. Amsterdam: Elsevier 1967; Katritzky, A. R., Lagowski, J. M.: Chemistry of the heterocyclic N-oxide. London: Academic Press 1971
2. Katritzky, A. R., Simmons, P.: Rec. Trav. Chem. **79**, 361 (1960); Tami, H., Fukushima, K.: J. Pharm. Soc. Japan **81**, 27 (1961); Katritzky, A. R., Randall, E. W., Sutton, L. E.: J. Chem. Soc. 1769 (1957); Sharpe, A. N., Walker, S.: J. Chem. Soc. 4522 (1961)
3. Chiang, J. F.: J. Chem. Phys. **61**, 1280 (1974)
4. Snerling, O., Nielsen, C. J., Nygaard, L., Pedersen, E. J., Sorensen, G. O.: J. Mol. Struct. **27**, 205 (1975)
5. Maier, J. P., Muller, J.-F.: J. Chem. Soc. Faraday Trans. II **70**, 1991 (1974)
6. Weimer, M. A., Lattman, M.: Tetrahedron Letters 1709 (1974)
7. Seibold, K., Wagnière, G., Labhart, H.: Helv. Chim. Acta **52**, 789 (1969)
8. Ito, M., Hata, N.: Bull. Chem. Soc. Japan **28**, 260 (1955)
9. Brand, J. C. D., Tang, K.-T.: J. Mol. Spectry. **39**, 171 (1971)
10. Hochstrasser, R. M., Wiersma, D. A.: J. Chem. Phys. **55**, 5339 (1971)
11. Yamakawa, M., T. Kuboda, T., Akazawa, H.: Theoret. Chim. Acta (Berl.) **15**, 244 (1969)
12. Kobinata, S., Nagakura, A.: Theoret. Chim. Acta (Berl.) **14**, 415 (1969)
13. Del Bene, J., Jaffé, H. H.: J. Chem. Phys. **49**, 1221 (1968)
14. Evleth, E. M.: Theoret. Chim. Acta (Berl.) **11**, 145 (1968)
15. Whitten, J. L.: J. Chem. Phys. **44**, 359 (1966)
16. Whitten, J. L.: J. Chem. Phys. **39**, 349 (1963)
17. Whitten, J. L., Hackmeyer, M.: J. Chem. Phys. **51**, 5584 (1969)
18. Hackmeyer, M., Whitten, J. L.: J. Chem. Phys. **54**, 3739 (1971)
19. Ha, T. K.: Mol. Phys. **27**, 753 (1974)
20. Ha, T. K., Wild, U. P.: Chem. Phys. **4**, 300 (1974)

21. Ha, T. K., Keller, L.: J. Mol. Struct. **27**, 225 (1975)
22. Ha, T. K.: Mol. Phys. **29**, 1829 (1975)
23. Petke, J. D., Whitten, J. L., Ryan, J. A.: J. Chem. Phys. **48**, 953 (1968)
24. Ha, T. K., O'Konski, C. T.: Intern. J. Quantum Chem. **7**, 609 (1973)
25. Mulliken, R. S., Person, W. B.: Molecular complexes. New York: Wiley 1969
26. Ha, T. K.: J. Mol. Struct. **30**, 103 (1976)
27. O'Konski, C. T., Ha, T. K.: J. Chem. Phys. **49**, 5354 (1968)
28. Kelly, H. P.: Phys. Rev. **180**, 55 (1969)
29. Kubota, T., Yamakawa, M., Mizuno, Y.: Bull. Chem. Soc. Japan **45**, 3282 (1972)

Received September 20, 1976